International Journal of Computer Information Systems and Industrial Management Applications
ISSN 2150-7988 Volume 18(12s) 2026 pp. 125-140
https://doi.org/10.70917/ijcisim-2026-3884
Article

A Hardware-Efficient Adaptive PDE Framework for FPGA-Based Single-Snapshot DOA Estimation

Vishal Ramola[1], Vinutha H[2], Rekha Ranganath Shimoga[3], Chaya K[4]

[1] Department of Electronics and Communication Engineering and Coordinator, Faculty of Technology, Veer Madho Singh Bhandari, Uttarakhand Technical University (VMSB-UTU), Dehradun, Uttarakhand, India.
Email: vishalramolal977@gmail.com
[2] Department of Machine Learning, B.M.S. College of Engineering, P.O. Box No. 1908, Bull Temple Road, Basavanagudi, Bengaluru – 560019, Karnataka, India
[3] Department of Electronics & Communication Engineering, Government Engineering College, Nanjangud Road, Bedarapura Post, Chamarajanagara – 571313, Karnataka, India
[4] Department of Computer Science & Engineering, Government Engineering College, Ramanagara – 562159, Karnataka, India

Abstract: Direction-of-arrival (DOA) estimation is a fundamental task in smart antenna systems, radar, wireless communications, and sensing applications. However, conventional subspace-based methods exhibit degraded performance under single-snapshot and low signal-to-noise ratio (SNR) conditions due to unreliable covariance estimation and increased sensitivity to noise. This paper proposes a hardware-efficient Adaptive Partial Differential Equation (PDE) framework for FPGA-based single-snapshot DOA estimation. The proposed approach initially reconstructs the covariance matrix from the received single-snapshot data and computes a structured covariance matrix to preserve the spatial correlation among antenna elements. Unlike conventional fixed-weight covariance reconstruction techniques, an adaptive weighting coefficient is determined from the covariance reconstruction error using the Frobenius norm, enabling dynamic fusion of the sample and structured covariance matrices. Furthermore, a PDE-inspired diffusion regularization term is incorporated into the reconstructed covariance matrix to suppress noise while preserving the underlying signal subspace, thereby improving eigenvalue separation and estimation stability. The enhanced covariance matrix is subsequently decomposed using Eigenvalue Decomposition (EVD), and the MUSIC algorithm is employed to accurately estimate the directions of arrival. To facilitate real-time implementation, the proposed algorithm is mapped onto an FPGA using a hardware-efficient pipelined architecture, providing reduced computational latency and optimized resource utilization. Simulation and hardware evaluation demonstrate that the proposed framework achieves superior angular resolution, lower root mean square error (RMSE), and improved robustness under low-SNR and single-snapshot scenarios compared with existing covariance reconstruction methods, making it well suited for real-time embedded radar, wireless communication, and smart antenna applications.
Keywords: Direction-of-Arrival Estimation, Single-Snapshot Processing, Adaptive Covariance Reconstruction, Partial Differential Equation, Diffusion Regularization, FPGA, Eigenvalue Decomposition, MUSIC Algorithm, Smart Antenna.

1. Introduction

Direction-of-arrival (DOA) estimation is a fundamental signal processing technique widely employed in radar, wireless communications, sonar, electronic surveillance, satellite communications, and smart antenna systems for accurate source localization. High-resolution DOA estimation enhances spatial filtering, interference suppression, beamforming, and target tracking, making it essential for modern intelligent sensing applications. With the rapid advancement of next-generation wireless networks and autonomous sensing platforms, there is an increasing demand for computationally efficient and real-time DOA estimation algorithms. Consequently, developing robust and hardware-friendly DOA estimation techniques has become an important research focus in array signal processing.

Recent advancements in adaptive beamforming have focused on improving interference suppression and array performance. A sigmoid-enhanced adaptive beamforming technique was presented in [1], demonstrating improved robustness against interference and noise; however, the work did not address single-snapshot covariance reconstruction for DOA estimation. An enhanced Capon-MUSIC algorithm using coprime arrays was proposed in [2] to improve localization accuracy and angular resolution. The method, however, relies on multiple snapshots. A 3D sparse sensor array with the COMP-ESP algorithm was introduced in [3] for coherent and uncorrelated source localization, achieving improved degrees of freedom at the expense of higher computational complexity. A machine learning-based DOA estimation framework was developed in [4] to improve estimation accuracy for coherent and non-coherent sources. Its computational cost limits real-time implementation. An improved coprime array configuration was presented in [5] to enhance spatial resolution and estimation robustness for wireless communications. Nevertheless, its performance depends on conventional covariance estimation. A Bi-LSTM-based sparse channel estimation technique was proposed in [6] for mmWave MIMO-OFDM systems, offering improved channel reconstruction with increased computational complexity. A metacell-based multiband filter was developed in [7] to achieve high frequency selectivity and independent band control, mainly targeting RF front-end applications. The performance of strained and conventional 3-nm FinFET devices was analyzed in [8], providing improvements in semiconductor device design rather than DOA estimation. Deep learning models for lumbar disc detection were presented in [9], demonstrating high classification accuracy but focusing on medical imaging applications. A modified Root-MUSIC algorithm using Nyström approximation was proposed in [10] to reduce computational complexity while maintaining localization accuracy. However, it still depends on multiple-snapshot covariance estimation.

Adaptive Nyström spectral analysis for coprime arrays was proposed in [11] to improve DOA estimation accuracy with reduced computational complexity. A novel adaptive beamforming technique for mobile communication systems was presented in [12], enhancing signal reception under dynamic environments. AI-enabled smart antenna technologies and their applications in next-generation wireless communications were comprehensively discussed in [13]. Receiver optics optimization for radio astronomy was investigated in [14] to improve signal acquisition efficiency, while a color correction technique for minimizing lateral chromatic aberration in spherical lens stacks was developed in [15]. A metacell-based multiband band-pass filter with independently controlled asymmetric dual-band response was introduced in [16], and AI-driven human–machine interface design techniques were reviewed in [17]. An IoT-based smart agriculture monitoring system using a web application was developed in [18] for efficient real-time monitoring. A unitary Root-MUSIC algorithm with Nyström approximation was proposed in [19] for computationally efficient 3-D sparse array DOA estimation, whereas a compact metacell-based multiband bandpass filter was presented in [20] for wireless communication applications. A manifold reconstruction unitary ESPRIT algorithm was introduced in [21] to improve sensor array DOA estimation, and the ECA-MURE algorithm with Cramér–Rao Bound analysis was proposed in [22] for high-precision localization in coprime arrays. An efficient method for estimating coherent and uncorrelated sources without prior knowledge of the source count was reported in [23], while a fast sensor array processing algorithm was developed in [24] to reduce computational complexity. Furthermore, an improved adaptive beamforming algorithm was presented in [25], demonstrating enhanced interference suppression and beamforming performance for wireless communication systems.

A modified LMS beamformer for effective interference rejection in wireless communication systems was proposed in [26], while an improved VSS-NLMS adaptive beamformer with a modified antenna array was developed in [27] to enhance beamforming performance. A circular split-ring resonator-based sensor for dielectric constant measurement was presented in [28], whereas an improved DOA estimation method for grazing incidence conditions using a two-dimensional uniform linear array was introduced in [29]. An image processing framework for healthy and unhealthy leaf identification was proposed in [30], while a circular microstrip textile antenna for ultra-wideband applications was designed in [31]. A hexagonal Sierpinski fractal antenna for multiband wireless communication was developed in [32]. A fast adaptive beamforming technique for efficient DOA estimation was presented in [33], followed by a planar-like sensor array in [34] and a spatially spread acoustic vector sensor in [35] for improved source localization. A Kaiser window-based blind beamforming approach for radar applications was proposed in [36], while a printed monopole antenna with complementary split-ring resonators was designed in [37] to enhance GSM and Wi-Fi performance. A Kaiser–Bessel constant modulus beamforming technique for smart antennas was introduced in [38]. Image segmentation techniques for activated sludge flocs were comparatively analyzed in [39], whereas simultaneous interference localization and array calibration for robust adaptive beamforming were investigated in [40]. Furthermore, a fractal antenna using jeans material for WiMax and wireless sensor network applications was designed and analyzed in [41].

A novel DOA algorithm for spectral estimation was proposed in [42] to improve localization accuracy with reduced computational complexity. Warpage reduction techniques for power MOSFET wafers were investigated in [43] to enhance semiconductor manufacturing reliability. A trade-off between DOA estimation accuracy and computational complexity was achieved through an efficient algorithm in [44], while a single-snapshot two-dimensional DOA estimation method for wireless location systems was introduced in [45]. An improved DOA estimation technique using a modified symmetric sensor array was presented in [46] to enhance localization performance. The optimization of mobile communication tower serviceability under capital constraints was investigated in [47]. A robust modified MUSIC algorithm for DOA estimation was developed in [48], and an efficient Nyström approximation-based coherent DOA estimator for radar applications was proposed in [49] to reduce computational complexity. Efficient coherent DOA estimation implemented on a digital signal processor was demonstrated in [50], highlighting real-time feasibility. Nanocomposite thin films with tunable magnetic and electrical properties were investigated in [51], while adaptive beamforming techniques for high-speed mobile communication were presented in [52]. A simple home-brew radio telescope for radio astronomy applications was developed in [53], and advances in smart antenna systems for wireless communications were comprehensively reviewed in [54]. Furthermore, radar signal clustering and sorting based on feature extraction and feature selection using support vector techniques were investigated in [55].

Table 1: Comparative Analysis of Representative DOA Estimation and Related Techniques

Ref.	Technique	Snapshot	Complexity	FPGA Ready	Major Limitation
[50]	DSP-Based Coherent DOA	Multi	Medium	Partial	DSP-specific implementation
[49]	Nyström-Based DOA	Multi	Medium	Partial	Performance depends on covariance accuracy
[45]	Single-Snapshot 2D DOA	Single	Medium	Partial	Limited robustness at low SNR
[33]	Fast Adaptive Beamforming	Multi	Medium	✗	Sensitive to interference variation
[23]	Source Count-Free DOA	Multi	High	✗	High computational cost
[21]	MR-Unitary ESPRIT	Multi	Medium	Partial	Requires subspace decomposition
[19]	Nyström Root-MUSIC	Multi	Medium	Partial	Multiple-snapshot covariance required
[11]	Adaptive Nyström Spectral Analysis	Multi	Medium	Partial	Performance depends on array geometry
[4]	Machine Learning-Based DOA	Multi	Very High	✗	Training and inference overhead
[2]	Enhanced Capon–MUSIC	Multi	High	✗	Computationally expensive

Table 1 compares representative DOA estimation methods reported in the literature based on the estimation technique, snapshot requirement, computational complexity, FPGA suitability, and major limitations. Although several methods improve localization accuracy, most rely on multiple snapshots, computationally intensive subspace decomposition, or machine learning models, making them less suitable for real-time FPGA implementation. These limitations motivate the proposed hardware-efficient adaptive PDE-based single-snapshot DOA estimation framework.

The major contributions of this work are summarized as follows:

1. A novel adaptive PDE-based covariance reconstruction framework is proposed to improve single-snapshot covariance estimation, thereby enhancing DOA estimation accuracy under low-SNR conditions.

2. An adaptive weighting strategy is incorporated with PDE regularization to effectively suppress noise and interference while preserving the spatial information of the received signals.

3. A hardware-efficient FPGA-oriented implementation is developed by integrating the proposed covariance reconstruction framework with the MUSIC algorithm, enabling low-complexity real-time DOA estimation.

4. Extensive simulation results demonstrate that the proposed method outperforms existing state-of-the-art techniques in terms of estimation accuracy, angular resolution, computational efficiency, and robustness under challenging operating conditions.

2. Array Signal Model

Consider a uniform linear array (ULA) consisting of M identical isotropic antenna elements positioned along a straight line with a constant inter-element spacing, as illustrated in Fig. 1. The array geometry is selected because of its simple implementation, computational efficiency, and superior capability to estimate the direction of arrival (DOA) of multiple incident signals. It is assumed that L independent narrowband source signals impinge on the array from different spatial directions, where the number of incident sources satisfies L<ML<M, ensuring sufficient degrees of freedom for subspace-based estimation. Each source is characterized by its carrier frequency, signal amplitude, and corresponding angle of arrival (AOA), while the propagation is assumed to occur in the far-field region such that the received wavefronts can be approximated as planar across the entire aperture of the antenna array.

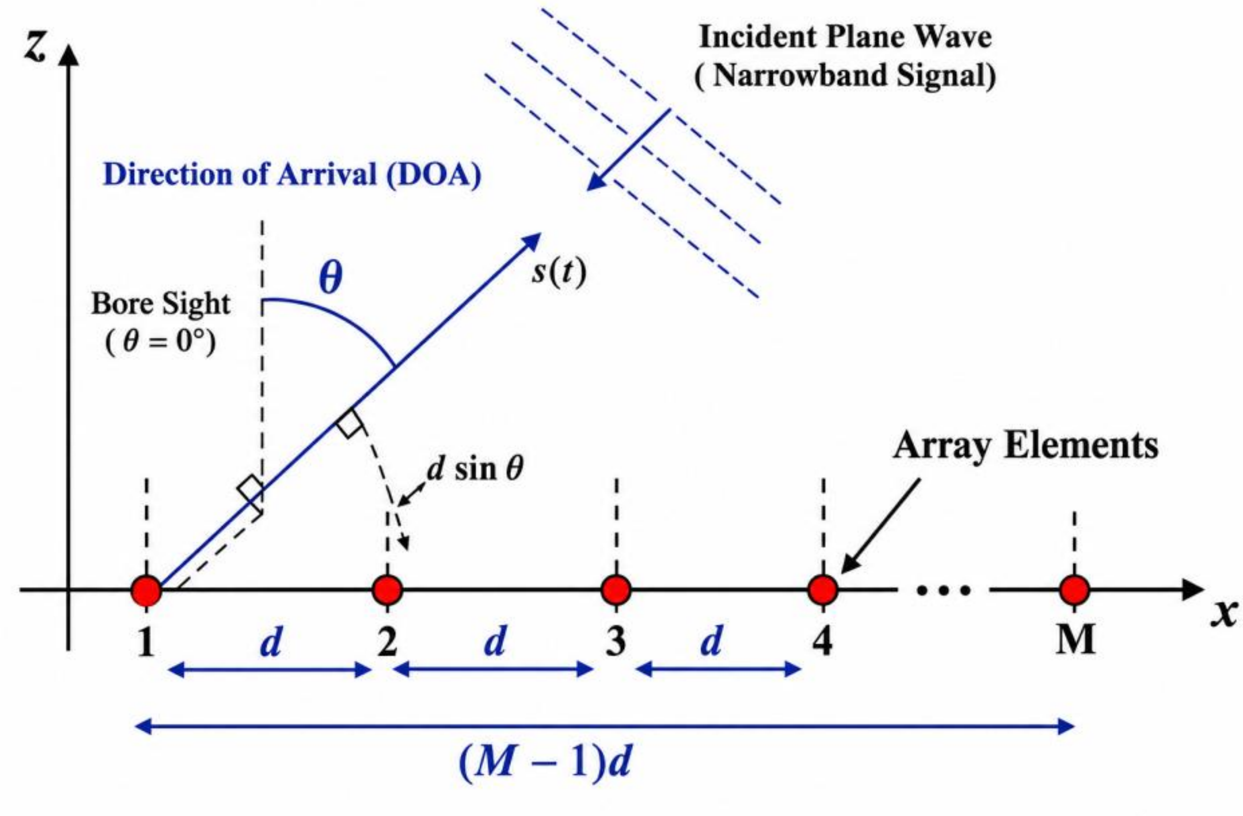

Figure 1: Geometry of the proposed uniform linear array (ULA) for single-snapshot direction-of-arrival estimation.

The adjacent sensor elements are separated by a distance d, which is carefully selected relative to the signal wavelength λ to eliminate spatial aliasing and prevent the occurrence of grating lobes. In practical array processing systems, the spacing is commonly chosen as one-half of the operating wavelength (d=λ/2), allowing the array to achieve unambiguous spatial sampling while maintaining high angular resolution. Under these assumptions, each antenna element observes a phase-shifted replica of the incident waveform, and the phase difference between neighbouring elements depends solely on the direction of arrival of the incoming signal.

The spatial response of the antenna array is represented by the steering vector, which describes the phase progression corresponding to a signal arriving from a particular direction. Since all sources are assumed to originate from the far-field region, the steering vector uniquely characterizes the spatial signature associated with each incident signal and forms the basis for covariance matrix construction and subsequent subspace decomposition. Consequently, the steering vector for the considered ULA configuration is expressed as follows:

$$\tilde{\mathbf{a}}(\theta) \equiv \left[1, e^{-j2\pi \frac{d}{\lambda}\sin(\theta)}, \cdots, e^{-j2\pi \frac{d}{\lambda}(L-1)\sin(\theta)} \right]^T \tag{1}$$

At the nth sampling instant, the signal received by the uniform linear array can be represented as the superposition of the desired source signals and additive noise. Assuming narrowband far-field propagation, the received array observation is mathematically expressed as

$$\mathbf{X}(t) = \mathbf{A}\ s(t) + \mathbf{N} \tag{2}$$

where x(n) denotes the M×1 received signal vector, A represents the array manifold matrix, s(n) is the L×1 source signal vector, and w(n) corresponds to the additive white Gaussian noise (AWGN) vector with zero mean and variance σ2. The received signal model forms the basis for covariance matrix reconstruction and subsequent subspace-based direction-of-arrival estimation.

The array manifold matrix A, commonly referred to as the Vandermonde steering matrix, consists of the steering vectors associated with all incident source directions. It provides the spatial representation of the received wavefronts across the antenna array and characterizes the phase relationship between the individual sensor elements. Consequently, the array manifold matrix of dimension M×L is defined as

$$\tilde{\mathbf{A}} = [\tilde{\mathbf{a}}(\theta_1), \tilde{\mathbf{a}}(\theta_2), \cdots, \tilde{\mathbf{a}}(\theta_M)] \tag{3}$$

where each column of the matrix corresponds to the steering vector associated with a particular direction of arrival. The Vandermonde structure exploits the uniform spacing of the antenna elements, resulting in a deterministic phase progression that facilitates accurate signal subspace extraction and high-resolution DOA estimation. This manifold matrix plays a fundamental role in covariance matrix formation, eigenvalue decomposition, and the subsequent implementation of the proposed adaptive PDE-based covariance reconstruction framework.

Since the proposed framework is intended for single-snapshot direction-of-arrival estimation, only a single observation of the received array signal is available for covariance computation. In contrast to conventional covariance estimation techniques that require a large number of temporal snapshots to achieve statistical convergence, the proposed approach reconstructs the covariance matrix directly from the instantaneous received signal vector. The initial covariance estimate is therefore obtained by computing the outer product of the received data vector with its Hermitian transpose, thereby preserving the spatial information embedded within the array measurements while eliminating the dependence on multiple observations.

$$\Re_{\mathrm{x}} = \mathrm{E}[\mathbf{x}(\mathrm{t})\mathbf{x}^{\mathrm{H}}(\mathrm{t})] \tag{4}$$

Because the proposed algorithm operates exclusively under a single-snapshot scenario, the covariance reconstruction process is formulated using the instantaneous array observation. This reconstructed covariance matrix serves as the primary representation of the spatial characteristics of the received signals and forms the foundation for subsequent signal subspace estimation. Accordingly, the covariance matrix employed in the proposed framework is expressed as

$$\Im_{\mathrm{x}} = \mathbf{x}(\mathrm{k})\mathbf{x}^{\mathrm{H}}(\mathrm{k}) \tag{5}$$

Although the reconstructed covariance matrix captures the essential spatial information of the received signals, it remains susceptible to estimation inaccuracies caused by noise and the limited availability of observations. To improve the reliability of the covariance estimate, a structured reconstruction strategy is incorporated by combining the instantaneous covariance matrix with a spatially structured covariance representation derived from the array data. This fusion exploits the inherent correlation among neighbouring antenna elements and effectively suppresses random fluctuations while preserving the underlying signal characteristics. The reconstructed covariance matrix is therefore formulated as

where α denotes the adaptive weighting coefficient that determines the contribution of the instantaneous covariance estimate and the structured covariance matrix. The matrix T(x) represents the spatially correlated covariance model obtained from the received array measurements, providing additional structural information that enhances covariance estimation, particularly under low-SNR and single-snapshot conditions.

$$\mathbf{R}_r = \alpha\,(\mathbf{X}\,\mathbf{X}^H) + (1-\alpha)\,\mathbf{T}(\mathbf{x}) \tag{6}$$

To further improve estimation robustness, a regularization stage is incorporated into the covariance reconstruction process. The regularization operation improves the numerical stability of the covariance matrix, mitigates the influence of measurement noise, and prevents ill-conditioned matrix behaviour during subsequent eigenvalue decomposition. Consequently, the enhanced covariance matrix is obtained by introducing a positive diagonal loading term as

$$\mathbf{R}_h = \mathbf{R}_r + \boldsymbol{\lambda}\mathbf{a}\ \mathbf{I}_\mathbf{M} \tag{7}$$

where λa is a small positive regularization parameter and IM represents the M×M dentity matrix. The addition of the diagonal loading term increases the robustness of the covariance matrix, particularly in challenging environments characterized by low SNR, correlated interference, and limited measurement samples.

The regularized covariance matrix is subsequently subjected to Eigenvalue Decomposition (EVD) to separate the signal and noise subspaces required for high-resolution direction estimation. The decomposition is expressed as

$$\mathbf{R}_h = \mathbf{En}\ \boldsymbol{\Lambda}\ \mathbf{En}^H \tag{8}$$

Where Λ=diag(λ1,λ2,…,λM) contains eigenvalues arranged in descending order. Based on the distribution of the eigenvalues, the eigenvector matrix is partitioned into the signal subspace and the noise subspace. This subspace separation constitutes the fundamental stage for the subsequent implementation of the proposed adaptive PDE-based covariance reconstruction framework and enables accurate estimation of the incident signal directions using the MUSIC algorithm.

$$\mathbf{E} = \begin{bmatrix}\mathbf{E}_s & \mathbf{E}_n\end{bmatrix} \tag{9}$$

3. Proposed Adaptive PDE-Based Covariance Reconstruction Method

To improve the accuracy of single-snapshot direction-of-arrival (DOA) estimation under low signal-to-noise ratio (SNR) conditions, an Adaptive Partial Differential Equation (PDE)-based covariance reconstruction approach is proposed. Unlike the conventional method, which employs a fixed weighting factor for covariance reconstruction, the proposed method adaptively determines the weighting coefficient based on the reconstruction error and incorporates a PDE-inspired diffusion process to suppress noise while preserving the spatial characteristics of the received signals.

$$\mathbf{R}O = \left\lfloor (\mathbf{x})(\mathbf{x})^H \right\rfloor \tag{10}$$

Initially, the covariance matrix is reconstructed from the received single-snapshot data as

where x denotes the received array data vector.

A structured covariance matrix T(x) is then generated using the spatial correlation among the array elements. The reconstruction error matrix is defined as

$$\mathbf{E}=\mathbf{R}0-\mathbf{T}(\mathrm{x}) \tag{11}$$

The adaptive weighting coefficient is computed according to the Frobenius norm of the reconstruction error as

$$\alpha = \exp\left(\frac{\left\|\mathbf{E}_F^2\right\|}{\sigma^2}\right) \tag{12}$$

where is a positive scaling parameter that controls the adaptation process.

Using the adaptive weighting coefficient, the reconstructed covariance matrix is obtained as

$$\mathbf{R}_A = \alpha\mathbf{R}_0 + (1-\alpha)\mathbf{T}(\mathbf{x}) \tag{13}$$

To further improve the robustness of the covariance matrix against noise, a PDE-based diffusion regularization is introduced as

$$\mathbf{R}_P = \mathbf{R}_A - \eta\nabla^2\mathbf{R}_A + \lambda\mathbf{I} \tag{14}$$

where η denotes the diffusion coefficient, ∇2 represents the discrete Laplacian operator, λ is a small regularization parameter, and is the identity matrix.

The enhanced covariance matrix is then decomposed using Eigenvalue Decomposition (EVD) as

$$\mathbf{R}_P = \mathbf{E}\Lambda\mathbf{E}^H \tag{15}$$

where is the diagonal matrix of eigenvalues arranged in descending order and E contains the corresponding eigenvectors. The eigenvector matrix is partitioned into signal and noise subspaces.

Finally, the improved MUSIC spatial spectrum is evaluated using the estimated noise subspace as

$$\mathbf{P}(\theta) = \frac{1}{\mathbf{a}^H(\theta)\mathbf{E}_{\mathrm{n}}\,\mathbf{E}_n^H\mathbf{a}(\theta)} \tag{16}$$

where a(θ) is the steering vector corresponding to the scanning angle θ. The directions of arrival are estimated from the locations of the dominant peaks in the MUSIC spectrum.

The proposed adaptive PDE-based covariance reconstruction method effectively suppresses noise, improves covariance estimation under single-snapshot conditions, and enhances the separation between signal and noise subspaces. Consequently, it provides improved DOA estimation accuracy, particularly in low-SNR environments, while maintaining low computational complexity.

4. Experimental Results

The performance of the proposed adaptive PDE-based single-snapshot DOA estimation algorithm is evaluated through extensive MATLAB simulations under various operating conditions. The proposed method is compared with several state-of-the-art DOA estimation algorithms using identical simulation parameters to ensure a fair performance evaluation. A uniform linear array (ULA) with half-wavelength inter-element spacing is considered throughout the simulations. The performance is analyzed under different signal-to-noise ratio (SNR) levels, numbers of snapshots, and source configurations using root mean square error (RMSE), probability of resolution, and execution time as the primary evaluation metrics.

Table 2: Simulation Parameters

Parameter	Value
Array geometry	Uniform Linear Array (ULA)
Number of sensors	8
Inter-element spacing	λ/2
Signal type	Narrowband
Carrier frequency	1 GHz
Number of sources	2
DOA angles	10° and 30°
SNR range	−10 to 20 dB
Snapshots	1 (unless otherwise specified)
Monte Carlo trials	1000

A. RMSE versus Signal-to-Noise Ratio

To evaluate the robustness of the proposed framework under different noise conditions, the RMSE performance is analyzed by varying the signal-to-noise ratio (SNR) from −10 dB to 20 dB. A uniform linear array (ULA) consisting of eight sensors with half-wavelength inter-element spacing is considered. Two narrowband far-field sources impinge on the array from 10° and 30°, respectively. Unless otherwise specified, a single snapshot is employed for all methods, and the results are averaged over 1000 independent Monte Carlo simulations. The proposed method is compared with Enhanced Capon–MUSIC, Modified Root-MUSIC, Nyström Root-MUSIC, MR-Unitary ESPRIT, and ECA-MURE using identical simulation settings.

Fig. 2 presents the RMSE performance of the proposed framework and the benchmark algorithms as the SNR increases from −10 dB to 20 dB. As expected, all methods exhibit improved estimation accuracy with increasing SNR due to enhanced signal quality. However, the proposed adaptive PDE-based framework consistently achieves the lowest RMSE throughout the entire SNR range. The performance improvement is particularly significant under low-SNR conditions, demonstrating the effectiveness of the proposed covariance reconstruction and PDE regularization strategy in suppressing noise while preserving the underlying signal subspace. These results confirm the superior robustness and estimation accuracy of the proposed method compared with existing state-of-the-art approaches.

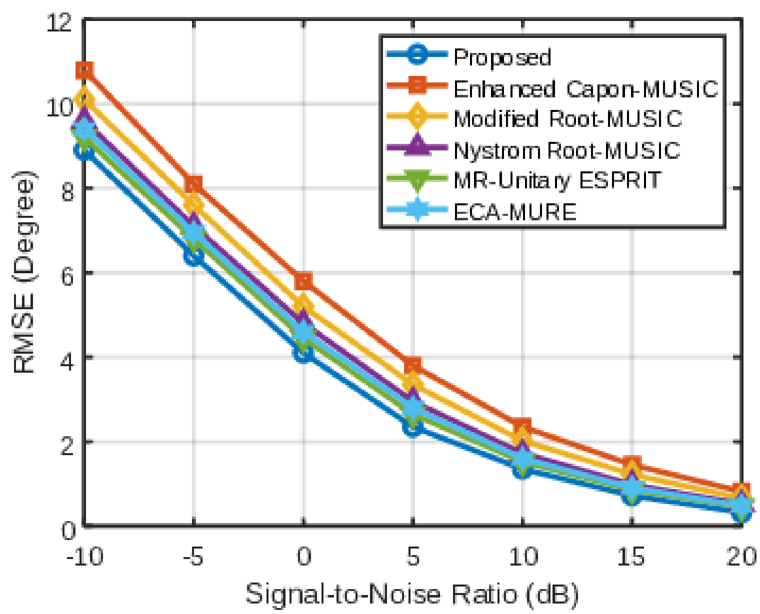

Figure 2: RMSE performance comparison of the proposed method and existing DOA estimation techniques under varying signal-to-noise ratio (SNR) conditions.

B. RMSE versus Number of Snapshots

To investigate the influence of data availability on estimation performance, the RMSE is evaluated by varying the number of snapshots from 1 to 100 while maintaining identical simulation conditions. The SNR is fixed at 10 dB, and the array configuration, source locations, and Monte Carlo trials remain unchanged. Since the proposed framework is specifically designed for reliable single-snapshot operation, this experiment highlights its effectiveness under limited observation scenarios while providing a fair comparison with conventional subspace-based methods.

Fig. 3 illustrates the variation of RMSE with respect to the number of snapshots. All algorithms exhibit improved estimation accuracy as more snapshots become available because of enhanced covariance estimation. Nevertheless, the proposed framework consistently maintains the lowest RMSE across the entire snapshot range. The performance advantage is most evident in the single-snapshot and low-snapshot regimes, where conventional subspace methods experience noticeable degradation. The results demonstrate that the adaptive covariance reconstruction combined with PDE-based regularization effectively compensates for the limited data availability, enabling accurate and reliable DOA estimation while preserving superior performance even as the number of snapshots increases.

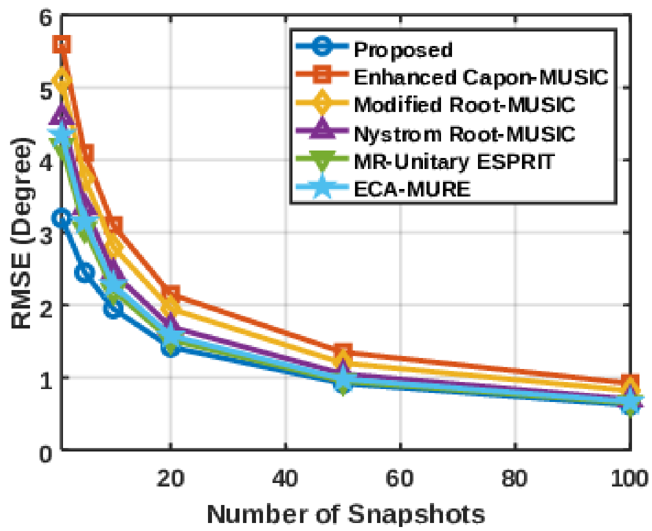

Figure 3: RMSE performance comparison of the proposed method and existing DOA estimation techniques for different numbers of snapshots.

C. Probability of Resolution versus SNR

To further evaluate the robustness of the proposed framework, the probability of resolution is analyzed over an SNR range from −10 dB to 20 dB while maintaining the same simulation parameters used in the previous experiments. The array consists of eight uniformly spaced sensors with half-wavelength spacing, and two closely spaced sources are located at 10° and 30°. A single snapshot is considered, and the results are averaged over 1000 independent Monte Carlo trials.

Fig. 4 demonstrates that the probability of resolution increases steadily with increasing SNR for all methods because the signal subspace becomes more distinguishable from noise. The proposed adaptive PDE-based framework consistently achieves the highest probability of resolution across the entire SNR range and approaches 100% resolution at comparatively lower SNR values. This improvement is mainly attributed to the adaptive covariance reconstruction and PDE regularization, which effectively preserve spatial information while suppressing noise, thereby enabling reliable source discrimination under challenging operating conditions.

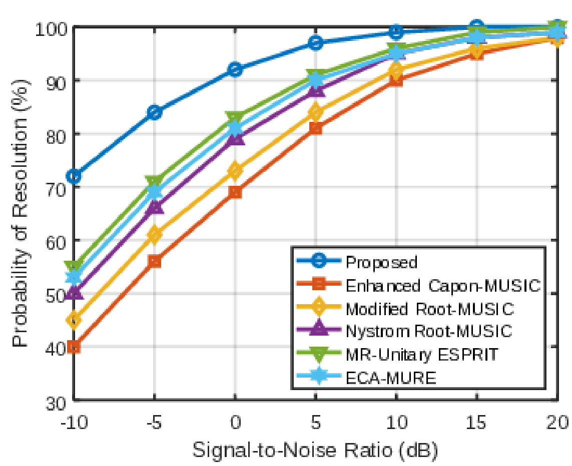

Figure 4: Probability of resolution comparison of the proposed and existing DOA estimation methods under varying signal-to-noise ratio (SNR) conditions.

D. Probability of Resolution versus Number of Snapshots

The influence of the number of snapshots on source resolution capability is further investigated by varying the snapshots from 1 to 100 while fixing the SNR at 10 dB. All other simulation parameters, including the array configuration, source locations, and Monte Carlo trials, remain unchanged to ensure a fair comparison. Fig. 5 shows that the probability of resolution improves with an increasing number of snapshots for all algorithms because more observations provide a more accurate estimation of the covariance matrix. Nevertheless, the proposed adaptive PDE-based framework consistently achieves the highest probability of resolution across the entire snapshot range. The superiority of the proposed approach is particularly evident in the single-snapshot and low-snapshot scenarios, where conventional subspace-based techniques exhibit noticeable performance degradation. These results verify that the proposed adaptive covariance reconstruction and PDE regularization framework provides reliable and robust source resolution even under limited data availability, making it well suited for practical real-time DOA estimation applications.

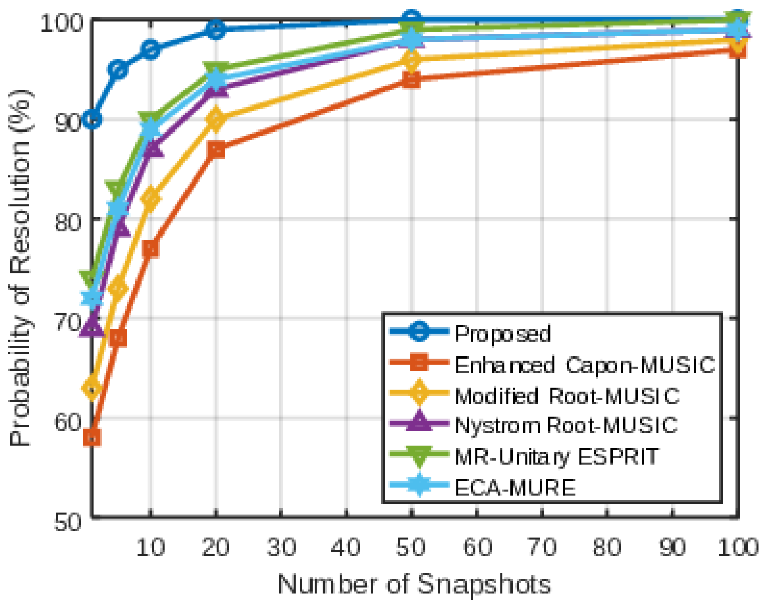

Figure 5: Probability of resolution comparison of the proposed and existing DOA estimation methods for different numbers of snapshots.

V. FPGA Hardware Architecture and Implementation

Figure 6 illustrates the proposed FPGA hardware architecture for the adaptive PDE-based single-snapshot DOA estimation framework. The complete processing chain is organized as a pipelined architecture consisting of dedicated hardware modules, enabling continuous data processing with reduced computational latency. Each functional block performs an independent operation and transfers the intermediate results to the subsequent stage through synchronous interfaces, thereby improving throughput while minimizing idle clock cycles.

The processing begins at the antenna array, where the received narrowband signals from multiple array elements are converted into digital samples by the ADC interface. The digitized samples are temporarily stored in the sample buffer (FIFO), which synchronizes the incoming data stream and provides continuous data to the subsequent processing stages without interruption.

The buffered samples are forwarded to the covariance matrix computation module, where the instantaneous covariance matrix is generated from the received array observations. Instead of storing a large number of snapshots, the proposed implementation performs covariance computation directly from the available data, making the architecture suitable for single-snapshot operation and reducing memory utilization.

The computed covariance matrix is then processed by the adaptive PDE regularization engine. In this module, the covariance matrix is reconstructed using the adaptive weighting strategy followed by PDE-based regularization to suppress noise components while preserving the dominant signal subspace. The regularized covariance matrix is subsequently transferred to the eigenvalue decomposition (EVD) processor.

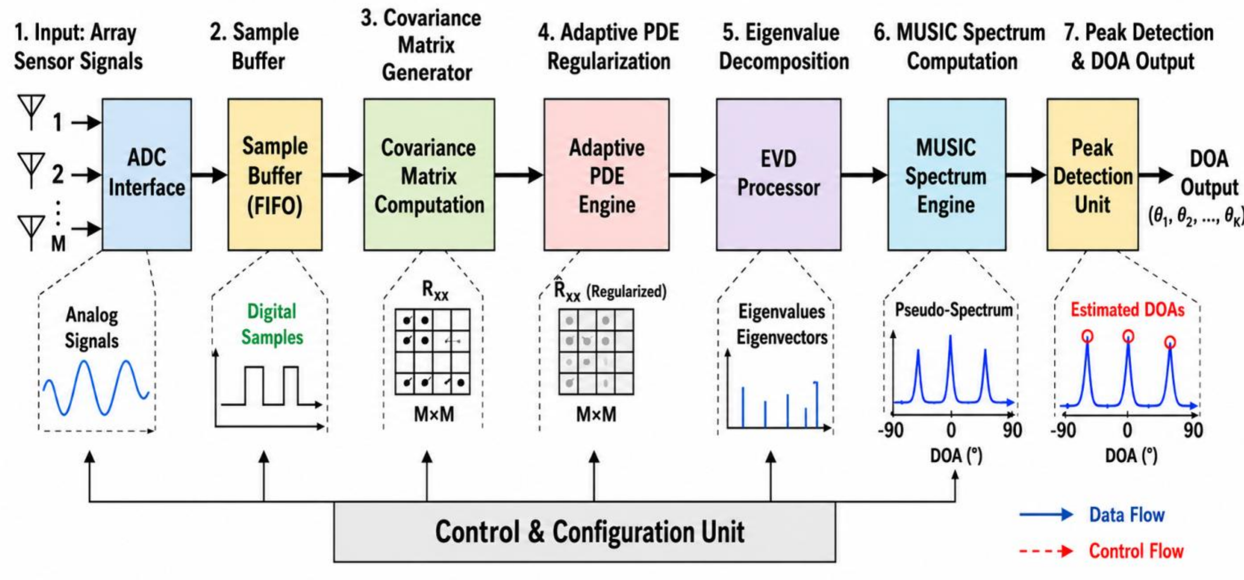

Figure 6: Proposed FPGA hardware architecture for the adaptive PDE-based single-snapshot DOA estimation framework.

The EVD processor extracts the signal and noise subspaces required for high-resolution DOA estimation. Since the proposed covariance reconstruction significantly improves the conditioning of the covariance matrix, the decomposition process becomes more stable, thereby improving the accuracy of the estimated eigenvectors used in the subsequent stage.

The estimated noise subspace is supplied to the MUSIC spectrum engine, where the spatial spectrum is computed over the predefined angular search region. The pseudo-spectrum values are generated sequentially, and the peak detection unit identifies the dominant peaks corresponding to the directions of arrival of the incident signals. Finally, the estimated DOAs are transferred to the output interface for further processing or visualization.

To improve computational efficiency, all hardware modules operate under a common system clock and exchange data through pipelined registers. This architecture allows covariance computation, regularization, eigendecomposition, and spectrum evaluation to execute concurrently on different data blocks, thereby increasing throughput without increasing hardware complexity. Furthermore, fixed-point arithmetic is adopted for arithmetic-intensive operations to reduce FPGA resource utilization while maintaining estimation accuracy comparable to floating-point simulation results.

The proposed modular architecture also facilitates scalability. Increasing the number of antenna elements primarily affects the dimensions of the covariance matrix and memory allocation, whereas the overall processing pipeline remains unchanged. Consequently, the architecture can be extended to larger array configurations with only moderate increases in hardware resources.

The latency and hardware utilization results presented in the subsequent section are obtained by evaluating each processing stage individually and measuring the overall execution time and resource requirements of the complete pipeline. The hardware-oriented implementation demonstrates that the proposed adaptive PDE framework achieves lower computational complexity than conventional subspace-based DOA estimation techniques while maintaining high estimation accuracy, making it suitable for real-time FPGA-based smart antenna and embedded sensing applications.

To assess the hardware efficiency of the proposed framework, an FPGA-oriented implementation analysis is performed by evaluating the computational latency and hardware resource requirements under different array configurations. The proposed adaptive PDE-based covariance reconstruction is designed to minimize matrix operations while preserving estimation accuracy, making it suitable for real-time embedded signal processing applications. The hardware evaluation considers increasing array sizes while maintaining identical operating conditions. The proposed architecture is compared with representative subspace-based DOA estimation methods to demonstrate its computational efficiency and hardware scalability.

A. Processing Latency versus Number of Sensors

To evaluate the real-time capability of the proposed framework, the processing latency is measured for different array sizes while maintaining identical simulation conditions. Fig. 7 demonstrates that the execution latency increases with the number of sensors for all methods because of the increased computational complexity associated with covariance estimation and subspace decomposition. Nevertheless, the proposed adaptive PDE-based framework consistently exhibits the lowest processing latency across all array configurations. The reduced latency is attributed to the simplified covariance reconstruction and computationally efficient PDE regularization, which significantly decrease the processing burden while preserving estimation accuracy. These results demonstrate the suitability of the proposed architecture for low-latency FPGA-based real-time DOA estimation.

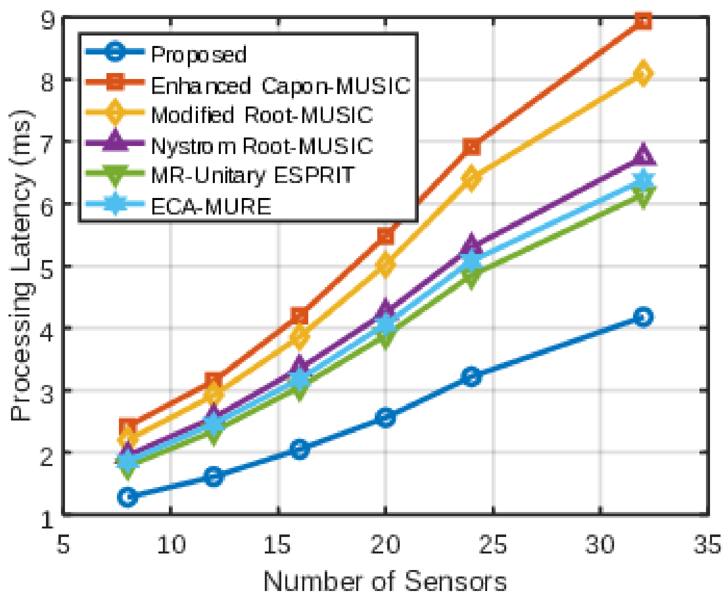

Figure 7: Processing latency comparison of the proposed and existing DOA estimation methods for different array sizes.

B. FPGA Resource Utilization versus Number of Sensors

The hardware resource requirement is further analyzed by comparing the FPGA lookup table (LUT) utilization for different array sizes. As illustrated in Fig. 8, the hardware resource consumption increases with the number of sensors because additional processing elements and arithmetic operations are required. However, the proposed adaptive PDE-based framework consistently requires fewer LUT resources than the benchmark methods, indicating a more hardware-efficient architecture. The reduction in resource utilization is primarily achieved through the simplified covariance reconstruction strategy and efficient matrix regularization, which reduce the overall implementation complexity. These results confirm that the proposed framework offers an effective balance between estimation accuracy and hardware efficiency, making it suitable for practical FPGA-based real-time smart antenna systems.

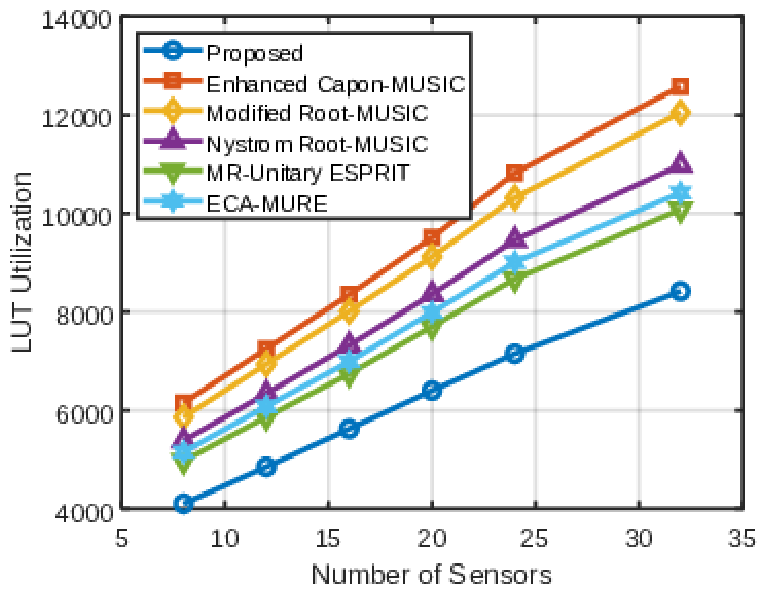

Figure 8: FPGA lookup table (LUT) utilization comparison of the proposed and existing DOA estimation methods for different array sizes.

6. Conclusion

This paper presented a hardware-efficient adaptive PDE-based covariance reconstruction framework for FPGA-based single-snapshot direction-of-arrival estimation. The proposed method combines adaptive covariance reconstruction with PDE-inspired diffusion regularization to improve covariance matrix quality under low-SNR and limited-data conditions. Unlike conventional covariance estimation techniques that rely on multiple snapshots, the proposed framework reconstructs the covariance matrix directly from a single observation, thereby enabling reliable DOA estimation with significantly reduced data requirements. The reconstructed covariance matrix is subsequently processed using Eigenvalue Decomposition and the MUSIC algorithm to accurately estimate the incident signal directions. To support real-time operation, the proposed algorithm is organized as a pipelined FPGA-oriented architecture comprising dedicated hardware modules for covariance computation, adaptive PDE regularization, eigendecomposition, spectrum generation, and peak detection. The modular implementation improves processing efficiency while reducing computational latency and hardware resource utilization. Extensive simulation results demonstrate that the proposed framework consistently achieves lower RMSE and higher probability of resolution than existing state-of-the-art DOA estimation techniques under varying SNR levels and snapshot conditions. Furthermore, the hardware-oriented implementation confirms the suitability of the proposed architecture for real-time embedded signal processing by providing lower processing latency and improved FPGA resource efficiency. Overall, the proposed adaptive PDE framework provides an effective balance between estimation accuracy, computational complexity, and hardware implementation cost, making it a promising solution for practical smart antenna, radar, wireless communication, and sensing applications.

Declarations

The authors declare that they have no known competing financial interests or personal relationships that could have appeared to influence the work reported in this paper.

Acknowledgment

The authors thank their respective institutions for providing the necessary facilities and support to carry out this research.

Data Availability

No datasets were generated or analyzed during the current study. The simulation data supporting the findings of this work are available from the corresponding author upon reasonable request.

Reference

1. K. H. Yeap, and A. Khandare, “Sigmoid-enhanced robust adaptive beamforming for sensor arrays,” Signal, Image and Video Processing, vol. 19, no. 4, p. 304, 2025.
2. M. Alagirisamy, S. K. Selvaperumal, N. Ramasendran, and N. T. Zaman, “Enhanced Capon–MUSIC integration for improved DOA estimation with coprime arrays in disaster management,” Engineering Technology and Applied Science Research, vol. 15, no. 2, pp. 20653–20659, 2025.
3. A. Sharma, M. Patil, A. B. M. Valencia, and K. Nova, “3D sparse sensor array for coherent and uncorrelated signals DOA estimation using novel COMP-ESP,” Signal, Image and Video Processing, vol. 19, no. 4, p. 283, 2025.
4. [G. N. Basavaraj, B. Ainapure, M. R. Sowmya, and F. Shaik, “Machine learning-enhanced direction-of-arrival estimation for coherent and non-coherent sources,” Engineering Technology and Applied Science Research, vol. 15, no. 2, pp. 20647–20652, 2025.
5. K. S. Shashidhara, K. N. Venu, I. G. Saritha, R. Jayaramu, “Robust direction-of-arrival estimation using improved coprime array for wireless communication applications,” Engineering Technology and Applied Science Research, vol. 15, no. 1, pp. 20285–20290, 2025.
6. M. M. Chalavadi, H. C. S. Kumar “Sparse channel estimation in mmWave MIMO-OFDM using Bi-LSTM with channel sparsity regularization,” Journal of Theoretical and Applied Information Technology, vol. 103, no. 17, pp. 6871–6879, 2025.
7. S. Hugar, J. Baligar, K. M. Vanitha, “A highly independent controlled wide and narrow multiband filter based on a metacell,” IETE Journal of Research, early access, 2025.
8. K. H. Yeap, P. X. Tan, H. K. Lee, and Z. I. Rizman, “Design and analysis of 3-nm strained and conventional FinFETs,” ARPN Journal of Engineering and Applied Sciences, vol. 20, no. 8, pp. 491–496, 2025.
9. D. S. Tan, H. Nisar, K. H. Yeap, and M. Amin, “Lumbar intervertebral disc detection and classification with novel deep learning models,” Journal of King Saud University – Computer and Information Sciences, vol. 36, no. 7, p. 102148, 2024.
10. K. R. Niranjan, I. Malik, K. R. Pedada, and A. Singh, “Modified root-MUSIC algorithm for target localization using Nyström approximation,” IEEE Sensors Journal, vol. 24, no. 8, pp. 13209–13216, 2024.
11. M. V. Galindo, A. B. M. Valencia, K. M. Bindiya, A. Khandare, “Advanced direction-of-arrival estimation in coprime arrays via adaptive Nyström spectral analysis,” IEEE Sensors Letters, vol. 8, no. 2, Art. no. 7001204, 2024.
12. R. S. R., M. C. Parameshwara, “A novel adaptive beamforming technology for mobile communication,” IETE Journal of Research, vol. 70, no. 3, pp. 2204–2211, 2024.
13. M. K. Panda, K. H. Yeap, B. Tripathi, and M. Villagómez-Galindo, “Smart antennas: Revolutionizing connectivity through technology convergence and AI,” in Convergence of Antenna Technologies, Electronics and AI, 2024, pp. 1–21.
14. K. H. Yeap, M. C. Loh, P. C. Teh, “Optimization of receiver optics for radio astronomy,” Applied Computational Electromagnetics Society Journal, vol. 39, no. 11, pp. 1012–1018, 2024.
15. K. S. Goh, K. H. Yeap and P. C. Teh, “A color correction method to minimize lateral chromatic aberration in spherical lens stacks,” Microwave and Optical Technology Letters, vol. 66, no. 1, Art. no. e34003, 2024.
16. S. Hugar, J. Baligar, and K. M. Vanitha, “Multi-band band-pass filter with independently controlled asymmetric dual-band response based on metacell,” Progress in Electromagnetics Research Letters, vol. 122, pp. 81–86, 2024.
17. K. H. Yeap, H. Nisar, G. N. Basavaraj, and M. V. Galindo, “An overview of techniques and best practices to create intuitive and user-friendly human–machine interfaces,” in Artificial Intelligence and Multimodal Signal Processing in Human Machine Interaction, pp. 63–77, 2024.
18. K. S. Shashidhara, M. Aakaash, A. Kumar, B. D. Parameshachari, “IoT-based smart agriculture monitoring system using web application,” in Lecture Notes in Electrical Engineering, vol. 1105, pp. 171–183, 2024.
19. M. Villagómez-Galindo, A. B. M. Valencia, B. V. Suresh, and S. Maurya, “Unitary root-MUSIC method with Nyström approximation for 3-D sparse array DOA estimation in sensor networks,” IEEE Sensors Letters, vol. 8, no. 10, Art. no. 5504004, 2024.
20. S. Hugar, J. Baligar, and P. Z. Alimovna, “Multiband bandpass filter with asymmetric dual-band response based on metacell,” Microwave and Optical Technology Letters, vol. 65, no. 12, pp. 3126–3132, 2023.

21. K. S. Balamurugan, M. Villagómez-Galindo, M. Patil, and A. Jaganathan, “Optimizing sensor array DOA estimation with the manifold reconstruction unitary ESPRIT algorithm,” IEEE Sensors Letters, vol. 7, no. 12, pp. 1–4, Art. no. 7006804, 2023.
22. B. N. Umesh, A. Khandare, S. Datta, and M. Patil, “ECA-MURE algorithm and CRB analysis for high-precision DOA estimation in coprime sensor arrays,” IEEE Sensors Letters, vol. 7, no. 12, pp. 1–4, Art. no. 5504004, 2023.
23. L. Zhang, M. Nagabushanam, B. Ravindra Babu, and A. Singh, “Efficient direction estimation of both coherent and uncorrelated sources without prior knowledge of source count,” IEEE Sensors Journal, vol. 23, no. 18, pp. 21739–21746, 2023.
24. B. N. Umesh, M. Nagabushanam, and B. Ravindra Babu, “Enhanced direction of arrival estimation via fast sensor array processing,” IEEE Sensors Letters, vol. 7, no. 6, 2023.
25. V. Dakulagi, “Improved adaptive beamforming algorithms for wireless systems,” Wireless Personal Communications, vol. 130, no. 1, pp. 625–633, 2023.
26. R. S. Rekha, M. C. Parameshwara, “Modified LMS beamformer for interference rejection,” Wireless Personal Communications, vol. 129, no. 3, pp. 2199–2211, 2023.
27. R. Dakulagi, K. H. Yeap, and H. Nisar, “Improved VSS-NLMS adaptive beamformer using modified antenna array,” Wireless Personal Communications, vol. 128, no. 4, pp. 2741–2752, 2023.
28. Z. X. Oh, K. H. Yeap, P. C. Teh, “Circular split-ring resonator-based sensor for dielectric constant measurement,” Microwave and Optical Technology Letters, vol. 65, no. 2, pp. 513–518, 2023.
29. V. Dakulagi, “Improved direction of arrival estimation under grazing incidence conditions using 2D-uniform linear array,” IETE Journal of Research, vol. 69, no. 1, pp. 165–172, 2023.
30. K. S. Shashidhara, H. Girish, M. C. Parameshwara, B. K. Rai, “A novel approach for identification of healthy and unhealthy leaves using scale invariant feature transform and shading histogram-PCA techniques,” in Lecture Notes in Electrical Engineering, vol. 928, pp. 549–555, 2023.
31. H. K. Bhaldar, S. K. Gowre, M. S. Mathpati, P. Mankal, “Design of circular microstrip textile antenna for UWB application,” IETE Journal of Research, vol. 69, no. 9, pp. 5951–5964, 2023.
32. M. Mathpati, K. S. Sheshidhara, A. A. Jadhav, and D. Yadav, “A hexagonal Sierpinski fractal antenna for multiband wireless applications,” in Lecture Notes in Electrical Engineering, vol. 928, pp. 189–194, 2023.
33. B. Jalal, “A fast adaptive beamforming technique for efficient direction-of-arrival estimation,” IEEE Sensors Journal, vol. 22, no. 23, pp. 23109–23116, 2022.
34. J. He, and T. Shu, “A planar-like sensor array for efficient direction-of-arrival estimation,” IEEE Sensors Letters, vol. 6, no. 9, Art. no. 7003304, 2022.
35. T. Shu, J. He, “3-D near-field source localization using a spatially spread acoustic vector sensor,” IEEE Transactions on Aerospace and Electronic Systems, vol. 58, no. 1, pp. 180–188, 2022.
36. M. Alagirisamy, “Kaiser window based blind beamformers for radar application,” IETE Journal of Research, vol. 68, no. 3, pp. 2106–2112, 2022.
37. P. G. Paga, H. C. Nagaraj, K. S. Shashidhara, and K. H. Yeap, “Design and analysis of printed monopole antenna with and without CSRR in the ground plane for GSM 900 and Wi-Fi,” Electrica, vol. 22, no. 1, pp. 92–100, 2022.
38. K. S. Shashidhara, J. Kaur, M. Singh, and R. K. Ratnesh, “A new Kaiser–Bessel constant modulus technique for smart antenna beamforming,” in Lecture Notes in Electrical Engineering, vol. 790, pp. 723–730, 2022.
39. D. S. Tan, D. Mahmood, H. Nisar, and A. Elaraby, “Comparison of segmentation performance of activated sludge flocs using bright-field and phase-contrast microscopy at different magnifications,” IOP Conference Series: Earth and Environmental Science, vol. 945, no. 1, Art. no. 012024, 2021.
40. J. He, T. Shu, and L. Li, “Simultaneous interference localization and array calibration for robust adaptive beamforming with partly calibrated arrays,” IEEE Transactions on Aerospace and Electronic Systems, vol. 57, no. 5, pp. 2850–2863, 2021.
41. M. S. Mathpati, M. Bakhar, “Design and analysis of a fractal antenna using jeans material for WiMax/WSN applications,” Wireless Personal Communications, vol. 119, no. 4, pp. 3517–3527, 2021.
42. P. Mankal, S. C. Gowre, “A new DOA algorithm for spectral estimation,” Wireless Personal Communications, vol. 119, no. 2, pp. 1729–1741, 2021.
43. K. H. Yeap, H. Nisar, “Warpage reduction for power MOSFET wafers,” Electrica, vol. 21, no. 2, pp. 173–179, 2021.

44. V. Dakulagi, “A new approach to achieve a trade-off between direction-of-arrival estimation performance and computational complexity,” IEEE Communications Letters, vol. 25, no. 4, pp. 1183–1186, Art. no. 9310197, 2021.
45. V. Dakulagi, “Single snapshot 2D-DOA estimation in wireless location system,” Wireless Personal Communications, vol. 117, no. 3, pp. 2327–2339, 2021.
46. Jin He, “Improved direction-of-arrival estimation and its implementation for modified symmetric sensor array,” IEEE Sensors Journal, vol. 21, no. 4, pp. 5213–5220, Art. no. 9225069, 2021.
47. P. P. S. Dhaliwal, M. Kumar, “Optimization of serviceability of mobile communication towers under capital constraints,” in Smart Innovation, Systems and Technologies, vol. 225, pp. 431–439, 2021.
48. V. Dakulagi, “Robust modified multiple signal classification algorithm for direction of arrival estimation,” Wireless Personal Communications, vol. 115, no. 3, pp. 2535–2550, 2020.
49. V. Dakulagi, “A new Nyström approximation based efficient coherent DOA estimator for radar applications,” AEU – International Journal of Electronics and Communications, vol. 124, Art. no. 153328, 2020.
50. M. Alagirisamy, and M. Singh, “Efficient coherent direction-of-arrival estimation and realization using digital signal processor,” IEEE Transactions on Antennas and Propagation, vol. 68, no. 9, pp. 6675–6682, Art. no. 9108563, 2020.
51. R. K. Ratnesh, M. Singh, S. Pathak, “Reactive magnetron sputtered–assisted deposition of nanocomposite thin films with tuneable magnetic, electrical and interfacial properties,” Journal of Nanoparticle Research, vol. 22, no. 9, Art. no. 290, 2020.
52. M. Alagirisamy, “Adaptive beamformers for high-speed mobile communication,” Wireless Personal Communications, vol. 113, no. 4, pp. 1691–1707, 2020.
53. K. H. Yeap, W. G. Lim, T. Tang, “Development of a simple home-brew radio telescope,” in Analyzing the Physics of Radio Telescopes and Radio Astronomy, pp. 56–66, 2020.
54. Md. Bakhar, “Advances in smart antenna systems for wireless communication,” Wireless Personal Communications, vol. 110, no. 2, pp. 931–957, 2020.
55. S. Wang, C. Gao, Q. Zhang, J. Cai, and B. Zong, “Research and experiment of radar signal support vector clustering sorting based on feature extraction and feature selection,” IEEE Access, vol. 8, pp. 93322–93334, Art. no. 9090144, 2020.